Journal of Magnetic Resonance 206 (2010) 200–204

Contents lists available at ScienceDirect

Journal of Magnetic Resonance

journal homepage: www.elsevier.com/locate/jmr

AnalyzeNNLS: Magnetic resonance multiexponential decay image analysis

Thorarin A. Bjarnason [a,*], J. Ross Mitchell [a,b,c,1]

[a] Radiology, Vancouver Coastal Health, Vancouver, Canada
[b] Clinical Neuroscience, University of Calgary, Calgary, Canada
[c] Radiology, University of Calgary, Calgary, Canada

ARTICLE INFO

Article history:
Received 27 February 2010
Revised 3 July 2010
Available online 16 July 2010

Keywords:
Magnetic resonance
Quantitative T_2
Matlab
Multiexponential analysis
Visualization

ABSTRACT

Exponential decays are fundamental to magnetic resonance imaging, yet adequately sampling and analyzing multiexponential decays is rarely attempted. The advantage of multiexponential analysis is the quantification of sub-voxel structure caused by water compartmentalization, with application as a non-invasive imaging biomarker for myelin. We have developed AnalyzeNNLS, software designed specifically for multiexponential decay image analysis that has a user-friendly graphical user interface and can analyze data from many MR manufacturers. AnalyzeNNLS is a simple, platform independent analysis tool that was created using the extensive mathematical and visualization libraries in Matlab, and released as open source code allowing scientists to evaluate, scrutinize, improve, and expand.

1. Introduction

Collecting and analyzing multiexponential decays using MRI allows quantification of sub-voxel structure due to water compartmentalization. Presently, multiexponential analysis of T_2 relaxation is used to measure myelin water fraction, an imaging biomarker of myelin, in peripheral [1] and central [2] nervous systems. Additionally, multiexponential analysis has revealed previously unknown inter-cellular water compartmentalization in pathological human brain [3,4]. Similar analyses have been performed using the longitudinal relaxation time (T_1) for NMR [5–9], and T_1–T_2 correlation MRI [10] and NMR [8,9,11] sequences.

However, amply sampling decays with MRI is both technically challenging and time consuming. There are two major hurdles: (1) scan times are lengthy and often provide information from only a single slice; and, (2) analysis of the resulting multiexponential decay data is complicated, difficult to replicate, and lacks integrated visualization of results. The latter limitation makes it difficult to correlate multiexponential decay patterns with anatomy, and to assess the impact of adjusting various algorithm parameters.

Research over the last several years has allowed development of new pulse sequences for multiexponential image data acquisition that reduce scan time while providing information from multiple adjacent slices [12,13]. These new pulse sequences may allow practical clinical application of a T_2 relaxation myelin imaging biomarker. However, data analysis methods have remained largely unchanged. Given that the new pulse sequences often produce significantly more data, and the growing interest in clinical use, the need for simple, reliable and standardized analysis becomes pressing.

Here we describe AnalyzeNNLS, a free, open source, platform independent software package that we hope will simplify, standardize, and advance multiexponential MRI research. We describe the algorithms used by AnalyzeNNLS and provide a feature overview by analyzing in vivo human data.

2. Background

Fitting multiexponential decays is an ill-posed problem and a challenging topic that has been reviewed comprehensively [14]. Multiexponential analysis is typically performed for MRI using the method outlined by Whittall and MacKay [15] based on the non-negative least squares algorithm of Lawson and Hanson [16]. The measured signal, y_i, can be characterized using a set of exponential basis functions describing [15]

$$y_i = \sum_{j=1}^{M} s_j e^{-t_i/T_{2j}}, \quad i = 1, 2, \ldots, N, \tag{1}$$

where t_i is the measurement time, M is the number of logarithmically spaced T_2 decay times, N represents the total number of data points, and s_j is the relative amplitude for each partitioned T_2 time, T_{2j}. The transverse relaxation time constant, T_2, can be replaced with

* Corresponding author. Address: Vancouver General Hospital, Department of Radiology, 899 West 12th Ave, Vancouver BC, Canada V5Z 1M9.
E-mail addresses: thor.bjarnason@coolth.ca (T.A. Bjarnason), rmitch@imaginginformatics.ca (J.R. Mitchell).
[1] Address: Imaging Informatics Laboratory, Heritage Medical Research Building, 3330 Hospital Drive NW, Calgary Alberta, Canada T2N 4N1.

1090-7807/$ - see front matter © 2010 Elsevier Inc. All rights reserved.
doi:10.1016/j.jmr.2010.07.008

the longitudinal relaxation time constant, T_1, depending on the measurement technique used. Similarly, for T_1–T_2 hybrid techniques Eq. (1) can be modified to include both T_1 and T_2 values according to Whittall [11]. The non-negative least squares (NNLS) algorithm [16] can be used, and sped up according to Andersson and Bro's [17] implementations of Bro and De Jong's `fastnnls` [18], to minimize χ^2.

Eq. (1) can be written in the general form such that

$$y_i = \sum_{j=1}^{M} A_{ij} s_j, \quad i = 1, 2, \ldots, N. \tag{2}$$

The NNLS algorithm is used to minimize

$$\chi^2_{\min} = \min \left[\sum_{i=1}^{N} \left| \sum_{j=1}^{M} A_{ij} s_j - y_i \right|^2 \right]. \tag{3}$$

The T_2 distribution, $S(T_2)$, is defined as the set of s_j for T_{2j}s, resulting from Eq. (3), and will comprise a set of delta functions. To better reflect biological microstructures, and to provide robust fits in the presence of noise, an additional smoothing constraint is added that minimizes the distribution curvature [15] by finding

$$\chi^2_{\mathrm{r}} = \min \left[\sum_{i=1}^{N} \left| \sum_{j=1}^{M} A_{ij} s_j - y_i \right|^2 + \mu \sum_{j=1}^{M} |s_{j+2} - 2s_{j+1} + s_j|^2 \right]. \tag{4}$$

Larger μ values favor smooth T_2 distributions over $\chi^2_{\min}$, while $\mu = 0$ gives $\chi^2_{\min}$. The optimal μ can be found using the generalized cross-validation approach [19,20].

The resulting T_2 distribution often consists of log-normal-like curves, with distinct peaks resulting from water compartmentalization. These peaks can be characterized by three factors: (1) area fraction; (2) geometric mean T_2 time (gmT_2), which is the mean T_2 time on a log scale; and (3) gmT_2 width ratio (gmT_2WR). The area fraction is determined by summing $S(T_2)$ within a desired region between $T_{2\min}$ and $T_{2\max}$ and dividing by the sum of all $S(T_2)$. The gmT_2 for a desired T_2 region is calculated as

$$\mathrm{gm}T_2 = \exp \left[\frac{\sum_{T_{2\min}}^{T_{2\max}} S(T_2) \log T_2}{\sum_{T_{2\min}}^{T_{2\max}} S(T_2)} \right]. \tag{5}$$

The gmT_2WR is determined by using the full width at half maximum (FWHM). By assuming the peak of interest is normal on a logarithmic scale, the FWHM can be found and the corresponding T_2 times, $T_{2\mathrm{long}}$ and $T_{2\mathrm{short}}$, can be defined as the T_2 times at the FWHM to the right and left of the peak, respectively. Then the gmT_2WR can be determined as [21]

$$\mathrm{gm}T_2\mathrm{WR} = T_{2\mathrm{long}}/T_{2\mathrm{short}}. \tag{6}$$

Since the T_2 distributions are discrete, the exact values of $T_{2\mathrm{long}}$ and $T_{2\mathrm{short}}$ might not exist. To compensate, $T_{2\mathrm{short}}$ uses the T_2 time with the amplitude to the left of the center of the peak and less than, but closest to, the FWHM. $T_{2\mathrm{long}}$ uses the T_2 time with the amplitude to the right of the center of the peak and greater than, but closest to, the FWHM. If the peak of interest is not log-normal-like, then gmT_2WR is not well defined. This type of assessment is best performed visually.

3. Features

3.1. Design considerations

There are two MRI multiexponential software options available [22,23], but both are costly and only work on Windows platforms. Following the works of van Beek [24] and Nilsson [25], we have developed a free, open source, platform independent software package that works independently of MR manufacturer.

Matlab [26] is a natural choice for this type of initiative. While not free, Matlab is an industry standard and most institutions provide Matlab access to their employees and students. Matlab is a matrix-oriented computation and visualization programming environment, with well established toolboxes for image processing, statistics, a graphical user interface (GUI) builder, and has an active community providing support in the newsgroups. The functionality of Matlab can easily be extended by writing custom toolboxes, and Matlab runs on most platforms, including Windows, Macintosh, and Linux.

AnalyzeNNLS has a simple and intuitive GUI, which can be seen in Fig. 1; only buttons that can be used at each stage are activated for the user. Similarly, the output displays of the analysis are hidden until after the data are analyzed, and buttons and panes are removed as necessary. The source code is open for scientists to evaluate, scrutinize, improve, and expand.

3.2. Design specifics

AnalyzeNNLS is capable of opening numerous single- and multi-slice file formats; including DICOM, data from Bruker (Bruker BioSpin Ltd.), GE (General Electric Company), and Varian (Varian Inc.), as well as the proprietary research formats MEID[2] and BFF.[3] Additional formats can be added by users as needed and included in the open source project.

AnalyzeNNLS allows users to save their work. At appropriate stages of analysis, users can either save ROIs, or all the results, for later recall. The results saved include: ROI; text files containing T_2 distributions; regional areas; gmT_2s; gmT_2WRs; decay; fit; residuals; and fitting information. All saved information can be loaded into AnalyzeNNLS for future recall. The results are saved as text files that are human readable and can easily be parsed using a scripting language in order to compile statistical data for large studies.

3.3. Analysis example

Fig. 1 shows an example of single-slice multiecho data immediately after loading into AnalyzeNNLS for determining multiexponential T_2 characteristics. At this stage users can window/level the image, scroll through slices or echoes, zoom in, load a new dataset or previously analyzed data, or draw and load ROIs.

Once an ROI is drawn, a panel appears to the right of the main window that displays a graph of the measured data and `Save ROI` and `Run NNLS` buttons are unveiled and can be seen in Fig. 2. The `Save ROI` button saves the ROI for future recall. Clicking `Run NNLS` launches the `Fitting Options` panel where users set appropriate parameters such as T_2 range and basis length, and echo start and cutoff. Once the parameters are set, the `Fit Data` button causes the `NNLS Fitting Options` panel to disappear while multiexponential data are analyzed.

Once the fitting routine completes, the three panels shown in Fig. 3 appear to the right of the main window and a results panel shown in Fig. 4 appears below the main window. To the right of the main window, the `Decay Data` panel is replaced with a panel that has the decay data along with the fit. The middle panel shows the residuals from the fit and the lower panel shows the T_2 distribution and cumulative sum. In the results panel below the main window users can change limits in the T_2 distribution in order to

[2] ImagingInformatics.ca MultiEcho Image Data file format, University of Calgary, Calgary, Canada.

[3] UBC MRI Research Centre file format, University of British Columbia, Vancouver, Canada.

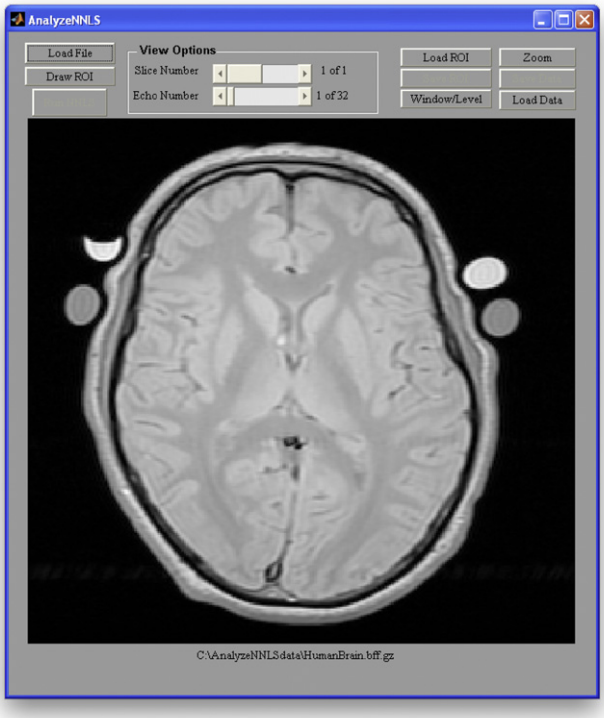

Fig. 1. AnalyzeNNLS immediately after MRI data are loaded. Note that buttons that are not usable at this stage are grayed out and non-functional. At this point users can window/level, scroll through slices or echoes, zoom in, load a new dataset or previously analyzed data, or draw and load ROIs.

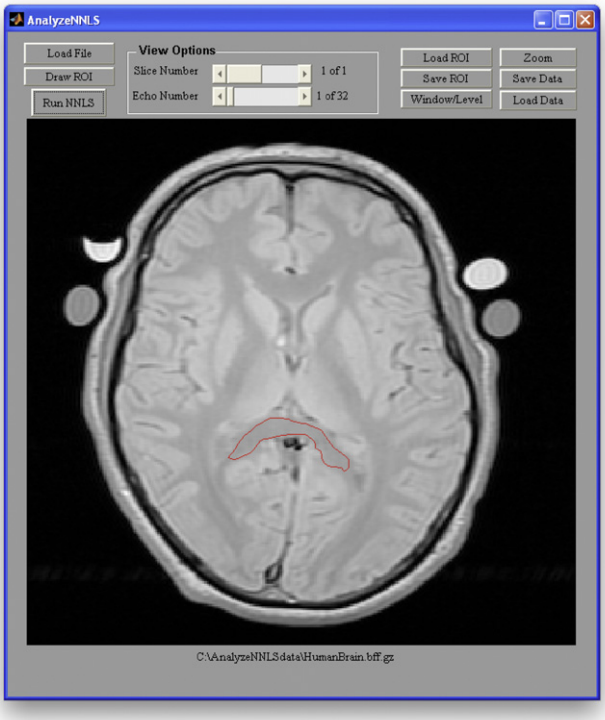

Fig. 2. Regions of interest are drawn using a function available in the Matlab image processing toolbox. Once the ROI is drawn an additional panel appears showing the decay of the signal averaged within the ROI for each echo (not shown). At this point more buttons are unveiled for further use.

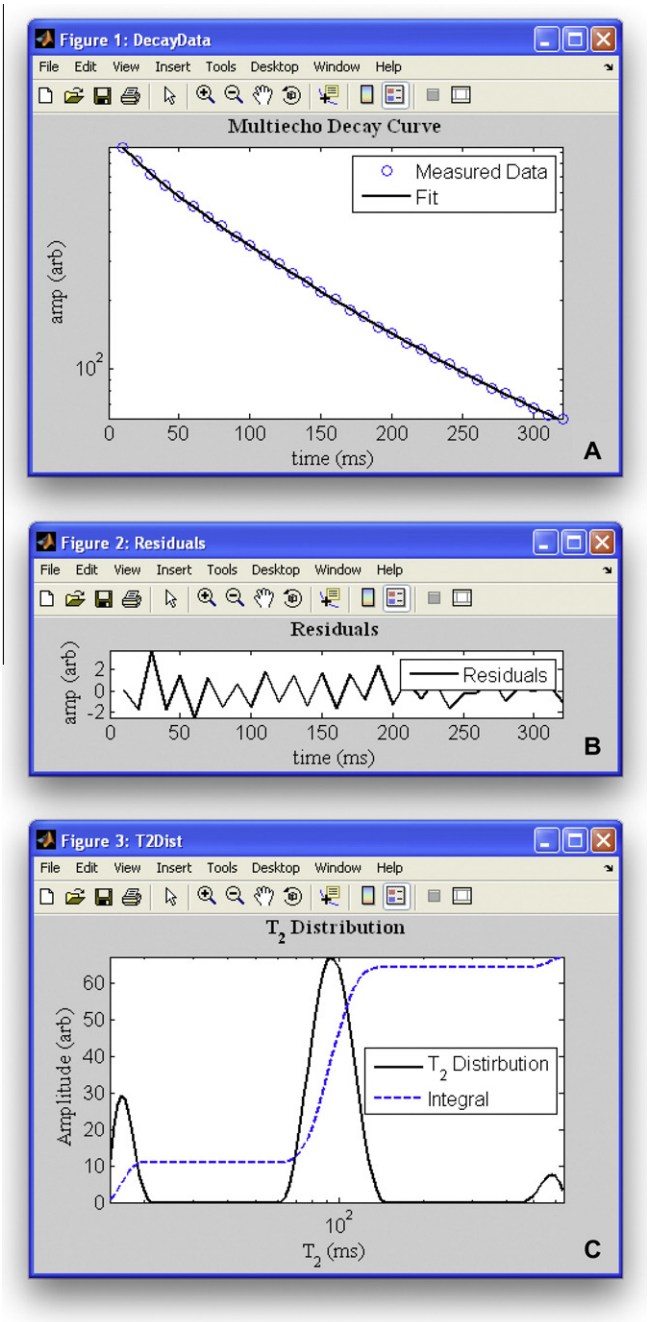

Fig. 3. Results panels appear to the right of the main window in the order shown. The decay and fit are depicted in A and the residuals of the fit are shown in B. The T_2 distribution and cumulative sum are displayed in C. Note, the oscillation in the residuals are not due to stimulated echoes, which would decrease with echo time, but are due to flow of nearby structures. No such oscillations were observed for ROIs in the minor forceps.

determine area fractions, gmT_2s, and gmT_2WRs. Data can be saved for future recall by using the `Save Data` button on the main window.

4. Discussion

Analyzing multiexponential decays using MRI is rarely attempted, yet these decays are fundamental to MRI. The advantage of collecting and analyzing multiexponential data is the quantification of sub-voxel compartmentalized microstructure. This type of analysis has been used as an imaging biomarker for myelin content

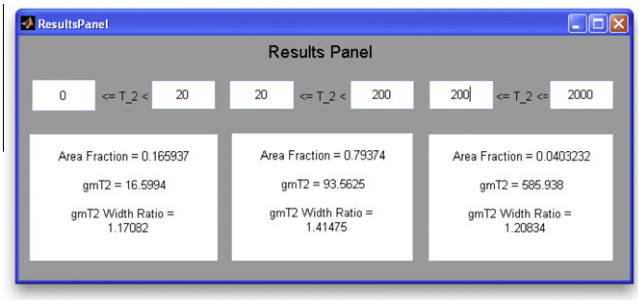

Fig. 4. Along with the results that appear as shown in Fig. 3, the Results panel appears below the main window. This panel allows users to modify the T_2 ranges in order to evaluate the area fractions, gmT_2s, and gmT_2WRs of T_2 distribution peaks in Fig. 3C.

[1,2] and has uncovered compartments yet to be classified in pathological brain [3,4].

Although only a human white matter example is shown here, multiexponential decays have been observed in other brain tissue, such as gray matter [13,27], ischemia [28], and tumor [29]. Multiexponential decays have been studied in: other biological tissue, such as blood [5], cervix [30], muscle [30], fat [30], breast [31], cartilage [32], liver [33], and prostate [34]; and physical structures such as wood [15,35], geophysical exploration of pore size in oil sands [36–38], and Renaissance wall paintings [39]. Of these various structures, AnalyzeNNLS has been used to study multiexponential decays in brain tissue (white and gray matter, ischemia, and tumor), muscle, cartilage, and cheese.

Collecting multiexponential decays with MRI is difficult and time consuming, and analyzing the resulting signal is nontrivial. We consider the possibility of sharing analysis software using open source an appreciable advantage for scientists that want to share results from multiexponential MRI studies. The usage of the analysis software described here facilitates the analysis and allows researchers to concentrate more on developing pulse sequences and experimental protocols.

The results obtained using AnalyzeNNLS can be saved for later recall so scientists can use familiar software to present their data. However, the graphs created using AnalyzeNNLS, shown in Fig. 3, use native Matlab plotting boxes intentionally, retaining built-in functionality such as zooming and the ability to edit the figure characteristics such as font, line type, and line width. Consequently, journal-quality figures can be created from the graphs in multiple image formats, such as eps, pdf, and tiff.

Presently, there are no open source software packages available for MR multiexponential analysis. There are many benefits to open source, it:

1. Allows scientists to review, improve, and update analysis methods collaboratively.
2. Gives scientists the opportunity to learn more about multiexponential analysis, and to come to their own conclusions as to whether or not the software is truly tailored to their needs.
3. Allows modification of the source code to repair errors and add features. These modifications can then be shared easily with other users.

AnalyzeNNLS is not meant to be an all-in-one MRI analysis solution, it is designed to do a specific task, multiexponential image analysis, well. If AnalyzeNNLS is not the exact tool required, scientists can keep the features they do need, and modify the source code accordingly. For instance, modifying the algorithm parameters in order to analyze the real portion of complex image data, as opposed to magnitude data, required changing two lines of code in the AnalyzeNNLS open source project. Furthermore, the fitting routines for AnalyzeNNLS are separated from the main GUI code, which makes it easy for users to experiment with novel multiexponential inversion algorithms.

5. Conclusion

Multiexponential decays are fundamental for MRI, and the acquisition and analysis of multexponential MR data is of growing importance. AnalyzeNNLS is free, open source software designed for magnetic resonance multiexponential decay image analysis that is capable of running on any operating system to analyze data from many MR manufacturers. Scientists are welcome to critique and improve AnalyzeNNLS by contributing to the open source project.

Acknowledgments

TAB and JRM are funded by the Alberta Heritage Foundation for Medical Research (now part of Alberta Innovates – Health solutions) and the Informatics Circle of Research Excellence (now part of Alberta Innovates – Technology Futures). Thank you to Cheryl McCreary for helpful feedback on the software and to Wendy Oakden, Craig Jones, and Shanrong Zhang for file-open scripts.

Appendix A

AnalyzeNNLS was written in Matlab [26], a platform independent, industry standard development environment with source code that is <400 kB when compressed. Matlab has various toolboxes ideal for image processing, including functions capable of displaying images, window/leveling, drawing ROIs, and curve fitting algorithms to name a few. Specifically, the image processing and statistics toolboxes are required to run and develop for this software.

AnalyzeNNLS is developed and distributed under the BSD license, allowing unlimited redistribution of the software. This project is hosted on sourceforge.[4] This contribution describes version 2.2.0 of AnalyzeNNLS running on Maltab 7.5.

A toolbox is available for Matlab that allows applications to be compiled for use on any operating system, and a linux version is available. End-users simply need to install the free Matlab Common Runtime to use a compiled application without a Matlab license. Since Matlab is platform independent, AnalyzeNNLS has been successfully used on Windows XP, Vista, and 7; Macintosh OS X 10.4–10.5; and Kubuntu and Red Hat Linux operating systems.

References

[1] E.E. Odrobina, T.Y.J. Lam, T. Pun, R. Midha, G.J. Stanisz, MR properties of excised neural tissue following experimentally induced demyelination, NMR Biomed. 18 (5) (2005) 277–284.
[2] C. Laule, P. Kozlowski, E. Leung, D.K.B. Li, A.L. MacKay, G.R.W. Moore, Myelin water imaging of multiple sclerosis at 7 T: correlations with histopathology, NeuroImage 40 (4) (2008) 1575–1580.
[3] S.M. Sirrs, C. Laule, B. Mädler, E.E. Brief, S.A. Tahir, C. Bishop, A.L. MacKay, Normal-appearing white matter in patients with phenylketonuria: water content, myelin water fraction, and metabolite concentrations, Radiology 242 (1) (2007) 236–243.
[4] C. Laule, I.M. Vavasour, B. Mädler, S.H. Kolind, S.M. Sirrs, E.E. Brief, A.L. Traboulsee, G.R.W. Moore, D.K.B. Li, A.L. MacKay, MR evidence of long T_2 water in pathological white matter, J. Magn. Reson. Imaging 26 (4) (2007) 1117–1121.
[5] R.S. Menon, P.S. Allen, Application of continuous relaxation time distributions to the fitting of data from model systems and excised tissue, Magn. Reson. Med. 20 (2) (1991) 214–227.

[4] http://sourceforge.net/projects/analyzennls.

[6] R.S. Menon, M.S. Rusinko, P.S. Allen, Proton relaxation studies of water compartmentalization in a model neurological system, Magn. Reson. Med. 28 (2) (1992) 264–274.
[7] M.D. Does, C. Beaulieu, P.S. Allen, R.E. Snyder, Multi-component T_1 relaxation and magnetisation transfer in peripheral nerve, Magn. Reson. Imaging 16 (9) (1998) 1033–1041.
[8] T.A. Bjarnason, I.M. Vavasour, C.L.L. Chia, A.L. MacKay, Characterization of the NMR behavior of white matter in bovine brain, Magn. Reson. Med. 54 (5) (2005) 1072–1081.
[9] T. Chandrasekera, J. Mitchell, E. Fordham, L. Gladden, M. Johns, Rapid encoding of T_1 with spectral resolution in n-dimensional relaxation correlations, J. Magn. Reson. 194 (1) (2008) 156–161.
[10] M.D. Does, J.C. Gore, Compartmental study of T_1 and T_2 in rat brain and trigeminal nerve in vivo, Magn. Reson. Med. 47 (2) (2002) 274–283.
[11] K. Whittall, Analysis of large one-dimensional and two-dimensional relaxation data sets, J. Magn. Reson., Ser. A 110 (2) (1994) 214–218.
[12] J. Oh, E.T. Han, S.J. Nelson, D. Pelletier, Measurement of in vivo multi-component T_2 relaxation times for brain tissue using multi-slice T_2 prep at 1.5T and 3T, Magn. Reson. Imaging 24 (1) (2006) 33–43.
[13] B. Mädler, S.A. Drabycz, S.H. Kolind, K.P. Whittall, A.L. MacKay, Is diffusion anisotropy an accurate monitor of myelination? Correlation of multicomponent T_2 relaxation and diffusion tensor anisotropy in human brain, Magn. Reson. Imaging 26 (7) (2008) 874–888.
[14] A.A. Istratov, O.F. Vyvenko, Exponential analysis in physical phenomena, Rev. Sci. Instrum. 70 (2) (1999) 1233–1257.
[15] K.P. Whittall, A.L. MacKay, Quantitative interpretation of NMR relaxation data, J. Magn. Reson. 84 (1) (1989) 134–152.
[16] C.L. Lawson, R.J. Hanson, Solving Least Squares Problems, Prentice-Hall, Englewood Cliffs, NJ, 1974.
[17] C. Andersson, R. Bro, The N-way toolbox for MATLAB, Chemom. Intell. Lab. Syst. 52 (1) (2000) 1–4.
[18] R. Bro, S. De Jong, A fast non-negativity-constrained least squares algorithm, J. Chemom. 11 (5) (1997) 393–401.
[19] G.H. Golub, M. Heath, G. Wahba, Generalized cross-validation as a method for choosing a good ridge parameter, Technometrics 21 (2) (1979) 215–223.
[20] A.N. Dula, D.F. Gochberg, M.D. Does, Optimal echo spacing for multi-echo imaging measurements of bi-exponential T_2 relaxation, J. Magn. Reson. 196 (2) (2009) 149–156.
[21] K.P. Whittall, Inversion of magnetic resonance data: How to T_2, 2006. <http://www3.telus.net/InversionsInc/t2.html> (Self published).
[22] V. Bortolotti, R.J.S. Brown, P. Fantazzini, UpenWin, 2009. <http://www.unibo.it/Portale/Ricerca/Servizi+Imprese/UpenWin.htm> (September 2009).
[23] Prospa. <http://www.magritek.com/prospa.html> (September 2009).
[24] J.D. van Beek, matNMR: a flexible toolbox for processing, analyzing and visualizing magnetic resonance data in Matlab, J. Magn. Reson. 187 (1) (2007) 19–26.
[25] M. Nilsson, The DOSY toolbox: a new tool for processing PFG NMR diffusion data, J. Magn. Reson. 200 (2) (2009) 296–302.
[26] Matlab. <http://www.mathworks.com> (September 2009).
[27] K.P. Whittall, A.L. MacKay, D.A. Graeb, R.A. Nugent, D.K. Li, D.W. Paty, In vivo measurement of T_2 distributions and water contents in normal human brain, Magn. Reson. Med. 37 (1) (1997) 34–43.
[28] M. Bruvold, J.G. Seland, H. Brurok, P. Jynge, Dynamic water changes in excised rat myocardium assessed by continuous distribution of $T1$ and $T2$, Magn. Reson. Med 58 (3) (2007) 442–447.
[29] L.R. Schad, G. Brix, I. Zuna, W. Härle, W.J. Lorenz, W. Semmler, Multiexponential proton spin–spin relaxation in MR imaging of human brain tumors, J. Comput. Assist. Tomogr. 13 (4) (1989) 577–587.
[30] C.S. Poon, R.M. Henkelman, Practical T_2 quantitation for clinical applications, J. Magn. Reson. Imaging 2 (5) (1992) 541–553.
[31] S.J. Graham, P.L. Stanchev, M.J. Bronskill, Criteria for analysis of multicomponent tissue T_2 relaxation data, Magn. Reson. Med. 35 (3) (1996) 370–378.
[32] L. Vidarsson, G.E. Gold, B. Hargreaves, J.M. Pauly, Linear combination filtering for T_2-selective imaging of the knee, Magn. Reson. Med. 55 (5) (2006) 1191–1196.
[33] M. Lupu, C.D. Thomas, J. Mispelter, Retrieving accurate relaxometric information from low signal-to-noise ratio ^{23}Na MRI performed in vivo, C. R. Chim. 11 (4-5) (2008) 515–523.
[34] T.H. Storåas, K.-I. Gjesdal, Ø.B. Gadmar, J.T. Geitung, N.-E. Kløw, Prostate magnetic resonance imaging: multiexponential T_2 decay in prostate tissue, J. Magn. Reson. Imaging 28 (5) (2008) 1166–1172.
[35] C.D. Araujo, A.L. MacKay, K.P. Whittall, J.R.T. Hailey, A diffusion model for spin–spin relaxation of compartmentalized water in wood, J. Magn. Reson. B 101 (1993) 248–261.
[36] W. Halperin, Application of spin–spin relaxation to measurement of surface area and pore size distributions in a hydrating cement paste, Magn. Reson. Imaging 12 (2) (1994) 169–173.
[37] J. Strange, Pore surface exploration by NMR, Magn. Reson. Imaging 21 (3–4) (2003) 221–226.
[38] K.E. Washburn, P.T. Callaghan, Tracking pore to pore exchange using relaxation exchange spectroscopy, Phys. Rev. Lett. 97 (17) (2006) 175502.
[39] N. Proietti, D. Capitani, E. Rossi, S. Cozzolino, A.L. Serge, Unilateral NMR study of XVI century wall painted, J. Magn. Reson. 186 (2007) 311–318.